Influence of Adding Mesocarbon Microbeads into C/C Composites on Microstructure and Properties during Carbonization

Hsien-Lin Hu,[1] Tse-Hao Ko,[1] Wen-Shyong Kuo,[2] Sung-Te Chen[3]

[1]*Department of Materials Science and Engineering, Feng Chia University, Taichung, Taiwan, Republic of China*
[2]*Department of Aeronautical Engineering, Feng Chia University, Taichung, Taiwan, Republic of China*
[3]*Department of Electronic Engineering, Hsiuping Institute of Technology, Taichung, Taiwan, Republic of China*

Received 13 May 2005; accepted 3 November 2005
DOI 10.1002/app.23745
Published online in Wiley InterScience (www.interscience.wiley.com).

ABSTRACT: This work tests the effect on microstructure, flexural strength, flexural moduli, plus the electrical and thermal conductivity of carbon/carbon composites with Mesocarbon Microbeads (MCMBs) content ranging 0–30% by weight during carbonization. These composites were reinforced by oxidative PAN Base fiber felts, and matrix precursor was resol-type-phenolic resin. MCMBs with a weight fraction of 0–30% were added to the matrix to elucidate the effect. Liquid-phase impregnation was applied to reinforce matrix carbon. Cured composites were stabilized at 230°C, then heat-treated at 400, 600, 800, 900 and 1000°C for carbonization. The measured flexural strength after heat-treated at 1000°C was 51.20, 49.59, 43.55, and 38.76 MPa for MCMBs with 0, 10, 20, and 30% added to composites; mean flexural moduli were l.73, 1.24, 0.73, and 0.57 MPa, respectively. Adding MCMBs reduced both strength and modulus because of cracks and avoids caused by different shrinkage between resin and MCMBs; adding 30 wt % MCMBs raised thermal conductivity of C/C composites from 1.55 to 1.78 W/mK and reduced electric resistivity from 1.8×10^{-2} to 5.97×10^{-3} Ω cm. J Appl Polym Sci 102: 3102–3110, 2006

Key words: composite; fiber; microstructure; pyrolysis; Raman spectroscopy

INTRODUCTION

Carbon/Carbon (C/C) composites have been an important area of research in recent decades owing to light weight, high thermal shock resistance, low thermal expansion, relatively high strength, and stiffness at high temperatures.[1–3] Pairing their excellent thermal shock and ablation resistance with their unique mechanical properties at high temperature allows the use of C/C composites in industry for manufacturing items such as brakes, nozzles, etc.; they are also appropriate as biomedical materials such as artificial joints by virtue of excellent bioaffinity and mechanical characteristics.[4,5] These composites exhibit appealing thermomechanical properties at high temperatures; their low resistance to oxidation in air is a major concern. Accordingly, several studies have attempted to develop coating technology for enhancing this oxidation resistance.[6–9]

The matrix of C/C composites can be derived from thermosetting phenolic resin or from thermoplastic pitch resin. Phenolic resin is widely employed as matrix precursor in forming C/C composites; they yield a large amount (40–50%) of carbon. Pitch resin is typically derived from coal-tar or petroleum; it is a complex mixture of numerous organic compounds with strong aromatic character. In contrast to C/C composites derived from pitch, most precursors exhibit higher thermal conductivity than those derived from thermosetting resin. One major limitation in using pitch resin as a matrix precursor to yield an adequate amount of carbon is depending on a very high pressure (up to 100 MPa) during processes of impregnation and carbonization.[10–12]

Mesophase was discovered by Brook and Taylor,[13,14] who found that the aromatic hydrocarbons from coal-tar, heavy oil residue, and pitch can slowly transform into mesophases during liquid phase carbonization. The mesophases exhibited anisotropic behavior (ordered structure), the original pitch matrix isotropic behavior (disordered), as revealed by polarized optical microscopy. Before bulk mesophases form, those mesophases present various mesophase spheres, which coarsen as smaller mesophase spheres combine during pyrolysis, before gradually transforming into bulk mesophase (nematic). Spheres, once separated from the matrix, are normally called mesocarbon micoobeads,[15] which had been considered an

Correspondence to: H.-L. Hu (watterhu@pchome.com.tw).
Contract grant sponsor: National Science Council, Republic of China; contract grant number: NSC 92–2216-E035–001.

TABLE I
The Characteristics of MCMBs [GCSMB (UH-01–07)] Extracted from Coal Tar

TI (Toluene insoluble) %	99.38 (JIS K 2425)
QI (Quinoline insoluble)%	99.52 (ASTM D2318)
Fixed carbon%	94.06 (ASTM D2415)
Average particle size (D_{50}, μm)	23.8 (Laser method)

excellent candidate raw material for making high-density carbons,[16] electrode materials for lithium ion rechargeable batteries.[17,18] MCMB was also used to manufacture high-performance carbon material, especially in terms of thermal and electrical conductivity.

Manocha et al.[19] and Ko[20] gauged cocarbonization of phenolic resin or oxidative PAN Base fibers to form C/C composites and saw complex chemical reactions and thermophysical changes occur at the fiber/matrix interface, affecting mechanical property and microstructure of C/C composites. Produced by the cocarbonization of phenolic resin and oxidative PAN Base fiber felt, C/C composites are low in cost, yet they show poorer thermal conductivity than materials derived from pitch precursors.

In this work, phenolic resin was first mixed with 0–30 wt % MCMBs as matrix precursors. Oxidative PAN Base fiber felts were subsequently cocarbonized to fabricate low-cost composites with high thermal and electrical conductivity.

EXPERIMENTAL

Raw materials

These C/C composites were reinforced by oxidative PAN Base fiber felts (Toho Rayon. Co., Japan), resol-type-phenol-formaldehyde resin (Chang Chum Petrochemical Industry Co., Taiwan) serving as matrix precursor. MCMBs (China Steel Chemical Co., Taiwan) were extracted from coal tar. Table I depicts characteristics of MCMBs.

Fabrication

As shown in Figure 1, oxidative PAN Base fiber felts were embedded in resins mixed homogenously with 0, 10, 20, and 30 wt % MCMBs for 30 min in a vacuum. The impregnated composites were cured at 80°C for 2 h and hot-pressed at 30 kg/cm^2 and 120°C for 30 min, then at 160°C for 10 min. Polymer composites were subsequently cut to appropriate size. Finally, cut samples were stabilized at 230°C and pyrolized at 0.5°C/min. up to 400, 600, 800, 900, and 1000°C for carbonization.

Measurements

A Rigaku X-ray Diffractometer with Cu Kα radiation sources verified d space and stacking size (L_C, stacking height of layer planes) of C/C composites. The Scherrer equation[21] yielded to calculate stacking size from width of the (002) reflection, B

$$L_C = \frac{k\lambda}{B\cos\theta} \tag{1}$$

in which $\lambda = 0.154$ nm; k is apparatus constant (= 1.0), and B is half-width of maximal intensity of the peak associated (002) reflection. Half-width of maximal intensity of this peak increases as stacking size (L_C) declines. Raman spectrum (Renishaw Raman imaging microscopy system) was utilized to ascertain microcrystalline planar size (L_a) and ratio of I_D/I_G (R), as follows:

$$R = \frac{I_D}{I_G} \tag{2}$$

$$L_a = 44\left(\frac{I_D}{I_G}\right)^{-1} \tag{3}$$

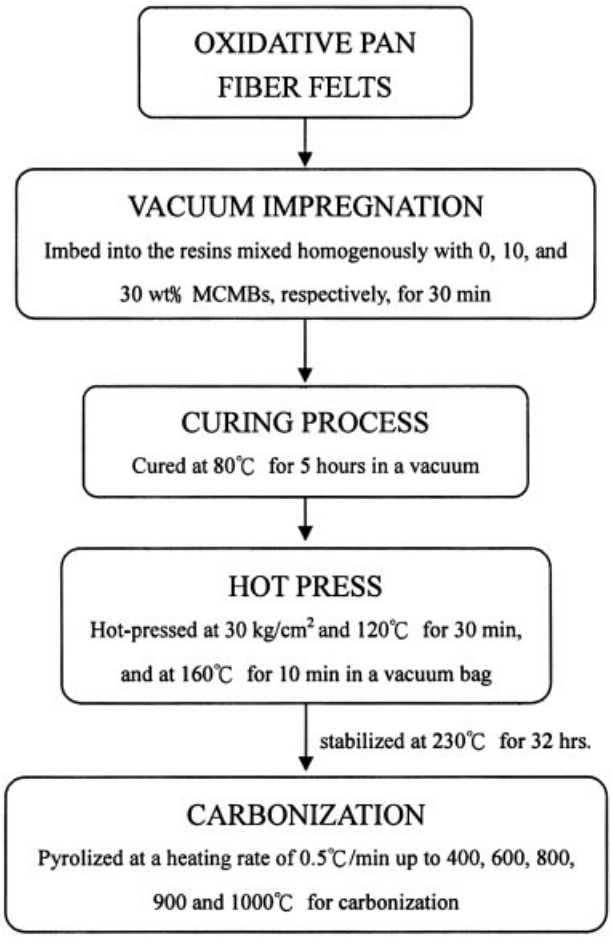

Figure 1 A flow diagram of carbon/carbon composites fabrication procedure.

where I_D is intensity of the peak at 1350 cm^{-1}caused by sp^3 bonding in carbon; I_G is intensity of the peak at 1890 cm^{-1} caused by sp^2 bonding in carbon.

Flexural strength (σ_b) and modulus (E_b) of C/C composites were determined by three-point bending method using ASTM 790 and relevant equations

$$\sigma_b = \frac{3P_{max}L}{2bt^2} \quad (4)$$

$$\text{and } E_b = \left[\frac{L^3}{4bt^3}\right]\left(\frac{p}{\delta}\right) \quad (5)$$

where P_{max} = maximum load (Kg); b = sample width (cm); t = samples thickness (cm); L = anvil distance (cm) (16× thickness), and P/δ = initial slope of stress-strain curves.

A scanning electron microscope (SEM, Hitachi S3000N, Japan) was employed to observe fracture morphology of composites; their polished surfaces were studied by reflection optical microscopy (OM) using an Olympus BHT apparatus. Texture of the aromatic layers with respect to the fiber and MCMB was determined under a crossed polarizer with a λ retarder plate.

Real density was measured by an AccuPyc 1330 Pycnometer in helium. Thermal conductivity was measured with a Micro300 (Holometrix, USA) according to ASTM 1461 C 714. Electrical resistivity and conductivity of composites were gauged by Mitsubishi Chemical MCP-T600 and four-point probes method; their open porosity measured according to ASMT D570.

RESULTS AND DISCUSSION

Physical changes during carbonization of precursor and polymer composites

The A, B, C, and D composites were derived from pure resin, from composite derived from resin mixing 10 wt % MCMBs, from composite derived from resin mixing 20 wt % MCMBs, and from composite derived from the resin mixing 30 wt %, respectively. Figure 2 plots the curves of weight loss of samples versus heat-treatment temperature.

Previous studies[22,23] considered chemical reactions and volatile species. Kimberly et al.[24] noted three reaction regions during the pyrolysis of the phenolic resin up to 1000°C. Figure 2 comprises three distinct regions: 230–400°C, 400–600°C, and 600–1000°C. The results of this work clearly show that the behaviors' correlation with weight loss during pyrolysis for composites is similar to that for the phenolic pure resin reported in the prior studies.[22–24] From 230 to 400°C, the weight loss slightly increased with temperature for all composites because water and low molecular

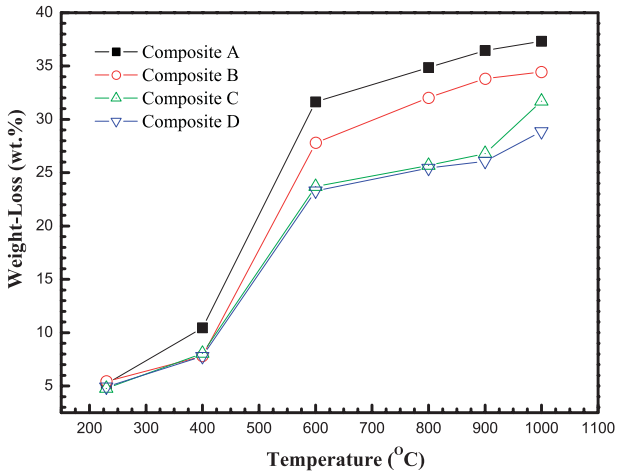

Figure 2 Weight loss variation of composite at different heat treatment temperatures. [Color figure can be viewed in the online issue, which is available at www.interscience.wiley.com.]

weight substances evolved in a condensation reaction in the resin encompassing methylene and hydroxyl functional groups, yielding the carbon-hydrogen crosslink.[22,23] In this phase, the crosslinking reaction between oxidative PAN Base fiber felts and phenolic resin also released a little water since these functional groups C—OOH, C—OH and C═O[25] on the oxidative PAN Base fibers' surface reacted with functional groups in a matrix to form strong interfacial bonding. Between 400 and 600°C, weight losses of composites A, B, C and D increased drastically because large volume of gases such as H_2O, CH_4, and H_2 evolved via condensation reaction in the cured resin.[22,23] Accordingly, the increase in rate of weight loss of composites decreased as the temperature rose above 600°C, since less water and species of smaller molecular weights, as well as H_2, CO and CO_2, were released.[22,23] In this phase, the hydrogen was identified as the dominant product, produced by splitting of the hydrogen atom directly bonded to benzene nuclei. Above 800°C, approximately 90% of the evolved gases were released. The weight losses of composite A, B, C, and D were 37.33, 34.45, 31.70, and 28.87 wt %, respectively, after heat-treatment at 1000°C.

Figure 3 records various composites shrinking continuously as temperature was raised to 1000°C. Unlike weight loss behavior of various composites, obviously, curves of shrinkage almost continually rose during carbonization. At less than 800°C, various composites shrank linearly with rise in temperature, owing to the condensation and crosslinking of the polymeric structure to form glassy carbon. Above 800°C, the rearrangement of carbon structure was the main cause of shrinkage, the rate of which declined. Meanwhile, it is also observed that the shrinkage of composites with MCMBs (composites B, C, and D) is

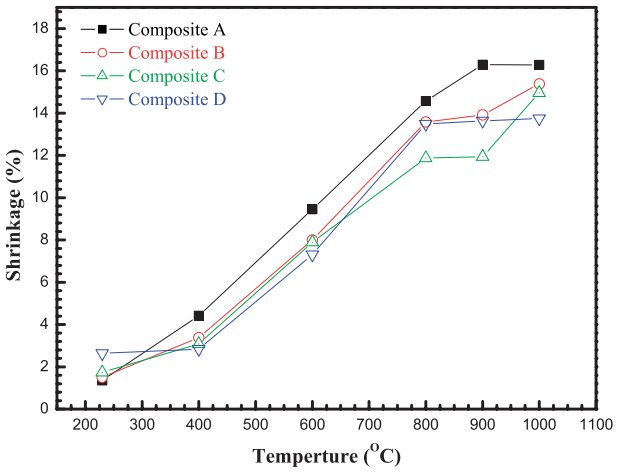

Figure 3 Shrinkage variation of composite at different heat treatment temperatures. [Color figure can be viewed in the online issue, which is available at www.interscience.wiley.com.]

smaller than that of a composite without MCMBs (composite A). Shrinkage of composite A, B, C, and D was 16.28, 15.38, 14.96, and 13.74%, respectively, at 1000°C.

Experiments revealed how adding MCMBs changes weight loss, shrinkage, and microstructure of glass-like carbon. Adding MCMBs retarded polymerization of resin, reduced weight loss, and limited shrinkage during heat-treatment. The decrease in carbonization weight loss and shrinkage with MCMBs added was noted. Weight loss and shrinkage of composite D improved by about 20 and 18%, respectively, over that of composite A.

Real-density and microporosity

Real density versus heat-treatment temperature is influenced by (1) dimensional change from shrinkage and (2) weight loss from evolution of volatile products during pyrolysis. Figure 4 maps changes in real density of composites. This study used an AccuPyc 1330 Pycnometer to calculate the real density of composites. For AccuPyc 1330 Pycnometer, pure helium gas was used to measure volume of composites. Initially, at 230, real density of all composites was in the range 1.28–1.33 g/cm^3. Above 230°C, polymeric structure of resin gradually transformed into glassy carbon structure. At the same time, evolved gases passed easily through pre-existing pores without expanding further and formed new open pores in the resin matrix. For density of all composites, chemical densification caused the density increase with heat-treatment temperature and the formation of new pores during pyrolysis resulted in density decreasing with heat-treatment temperature. These two reactions competed with each other during pyrolysis process. In Figure 4, the small decreases in density for all composites were observed at 230–400°C. Thus, the formatting new pore reaction was regarded as an important factor in affecting the density of composites in this phase. The real density of composites B, C, and D rose sharply between 400 and 1000°C; the increase for composite D was maximal, from 1.34 to 1.69 g/cm^3; that of composite C was moderate, from 1.32 to 1.64 g/cm^3; and that for composite B was minor, from 1.28 to 1.63 g/cm^3. Composite A exhibited a smaller increase from 400 to 600°C, but a sharply increase above 600°C. At 900°C, the real density of composite A also fell abruptly because of formation of closed micropores in the phenolic resin matrix. As a results, the chemical reaction was regarded as an important factor to affect the density for all composites above 400°C. At 1000°C, final real density of composite A was 1.53 g/cm^3; for B, 1.63 g/cm^3; for C, 1.64 g/cm^3; and for D, 1.69 g/cm^3.

Figure 5 plots variation in fractional volume of open porosity of composites with temperature of heat-treatment. Initially at 230°C, friction volume of open pores was 1.88% for composite A, 1.85% for B, 1.83% for C, and 1.85% for D. The friction volume of open pores of all composites increased rapidly between 400 and 600°C because of formation of great amounts of avoids and cracks caused by volatile gas from resin. At 600–900°C, increase rate of various composites became moderate, since aromatization and crosslinking among heterocyclic rings, plus lengthening and broadening of carbon based planes, led to repacking of structure in resin. Above 900°C, the friction of pores for all composites raised sharply again, with pore size expanded by nitrogen gas from PAN fibers. At 1000°C, friction volumes of open porosity of composites A, B, C, and D was 9.24, 9.98, 10.11, and 10.66%, respectively.

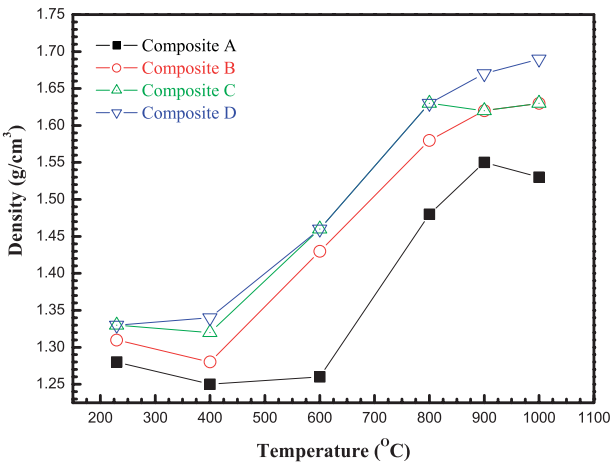

Figure 4 The results of change in real density in composites at different heat treatment temperatures. [Color figure can be viewed in the online issue, which is available at www.interscience.wiley.com.]

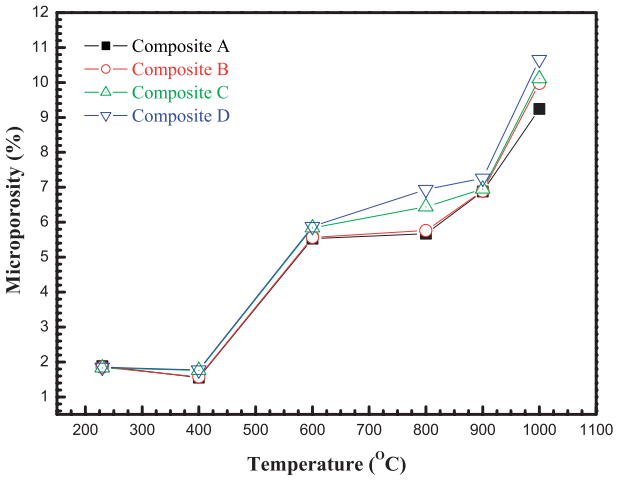

Figure 5 The result of change in friction volume of open-pores in composites at different heat treatment temperatures. [Color figure can be viewed in the online issue, which is available at www.interscience.wiley.com.]

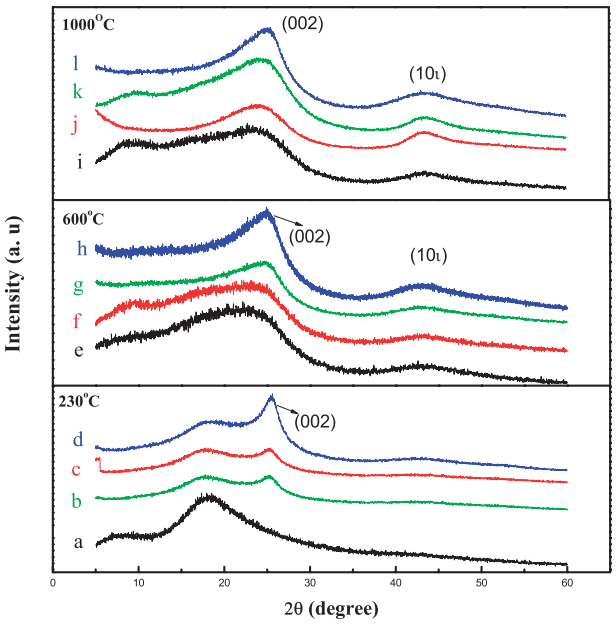

Figure 6 The change in X-ray Diffraction pattern of composites at different heat treatment temperatures: (a) composite A at 230°C, (b) composite B at 230°C, (c) composite C at 230°C, (d) composite D at 230°C, (e) composites A at 600°C, (f) composite B at 600°C, (g) composite C at 600°C, (h) composite D at 600°C, (i) composite A at 1000°C, (j) composite B at 1000°C, (k) composite C at 1000°C, (l) composites D at 1000°C. [Color figure can be viewed in the online issue, which is available at www.interscience.wiley.com.]

Differences in shrinkage of MCMB versus phenolic resin matrix cause formation of numerous pores and cracks around MCMBs, which explains why friction volume of pores in composites B, C, and D exceeds that of composite A.

X-ray diffraction and Raman spectra

In the X-ray diffraction pattern of carbon material, peaks, (002), (004), (004), (101) and (110) reveal crystalline order in carbon.[26] Figure 6 displays X-ray patterns for a composite following pyrolysis at various temperatures. In Figure 6(a), for cured composite A (heat-treated at 230°C), a broad peak at 2θ from 17.5 to 22.7° corresponds to polymer structure in phenolic resin; this peak is associated with the chain adjacent to the linear polymer after resin cured.[27] Another weak peak at $2\theta \approx 9.7°$ also corresponds to phenolic resin. At the same time, for composites with MCMBs (composite B, C, and D), a peak at $2\theta \approx 25.5°$ was observed, due to adding MCMBs into resin; this peak corresponds to a (002) reflection for carbon, as shown in Figure 8. For composite A, a broad peak at 2θ between 17.5 and 22.7° began to shift to 25.4° and became narrow and sharp as heat-treated temperature rising, due to polymer structure for resin transferring gradually to glasslike carbon. Above 800°C, a weak peak at $2\theta \approx 47.5°$ corresponds to (101) reflection for carbon; it also became narrow and sharp with raising temperature. For these composites with MCMBs, intensities of peaks corresponding to (002) and (101) reflection for carbon increased and half-width of the peak of the (002) basal plane of the carbon to decline with temperature of heat treatment. Adding MCMBs caused intensity of peaks of the (002) and (101) planes to rise faster with temperature.

Table II lists stacking sizes (L_C), temperatures, L_C values tabulated according to Equation 3. Table III indicates that L_C values are a function of temperature,

TABLE II
Thermal Conductivity and Electric Resistance for Composites A, B, C, and D after Carbonization at Temperature 1000°C and Results of L_C and L_a for Composite with HTT

	Composite A		Composite B		Composite C		Composite D	
Temperature (°C)	L_C (nm)	L_a (nm)	L_C (nm)	L_a (nm)	L_C (nm)	L_a (nm)	L_C (nm)	L_a (nm)
600	0.857	0.752	0.882	1.392	0.917	1.532	0.963	1.681
800	0.971	0.939	0.974	1.214	1.014	1.348	1.134	1.382
900	1.14	0.984	1.165	1.287	1.186	1.357	1.227	1.442
1000	1.71	1.138	1.391	1.294	1.412	1.363	1.523	1.83

TABLE III
Thermal Conductivity and Electric Resistance for Composites A, B, C, and D after Carbonization at Temperature 1000°C

Sample	Thermal conductivity (W/mK)	Electric resistance (Ωcm)
Composite A	1.55	1.8×10^{-2}
Composite B	1.57	6.7×10^{-3}
Composite C	1.65	6.1×10^{-3}
Composite D	1.78	5.97×10^{-3}

associated with generation of isotropic structures. Adding MCMBs increased L_C effectively. At 1000°C, L_C for composites A, B, C, and D was 1.36, 1.27, 1.39, and 1.52 nm, respectively.

In this work, a Raman spectrum associated with $\lambda = 632.8$ nm obtained with a 25W He–Ne laser is considered to typify microstructure. Equations 2–3 specify ratio of I_D/I_G (R) and microcrystalline planar size (L_a). Figure 7 shows fitted Raman spectra of various composites at 1000°C: two strong wide bands near 1580 and 1360 cm^{-1}. A peak near 1580 cm^{-1} was associated with graphitic structure (D band), and that near 1360 cm^{-1} with disordered structure (G band) in carbon. Increase in order in carbonaceous materials is well known to be reflected by increased frequency of the G mode and/or decreased frequency of D mode. A Table II also provides the variations in the microcrystalline planar size (L_a) of composites A, B, C, D, above 600°C. The L_a of composite A rose smoothly from 0.75 to 1.14 nm as pyrolysis temperature rose from 600 to 1000°C. From 600 to 800°C, the evolution of gas, especially hydrogen, distorts the basal plane associated with carbon of MCMBs. Accordingly, the value of L_a, length of basal plane for carbon, is reduced and the basal plane of carbon begins to be rearranged above 800°C. At 800°C, L_a value of composites B, C, and D are lower than that of composite A. As the temperature increases from 900 to 1000°C, L_a values of these composites with MCMBs barely changes. At 1000, L_a value is 1.14 for composite A; composites B, C, and D showed 1.29, 1.36, and 1.8 nm, respectively. L_a and L_C values of composites with added MCMBs (composites B, C and D) exceeded those of composite A because of high density and good crystalline of MCMB.

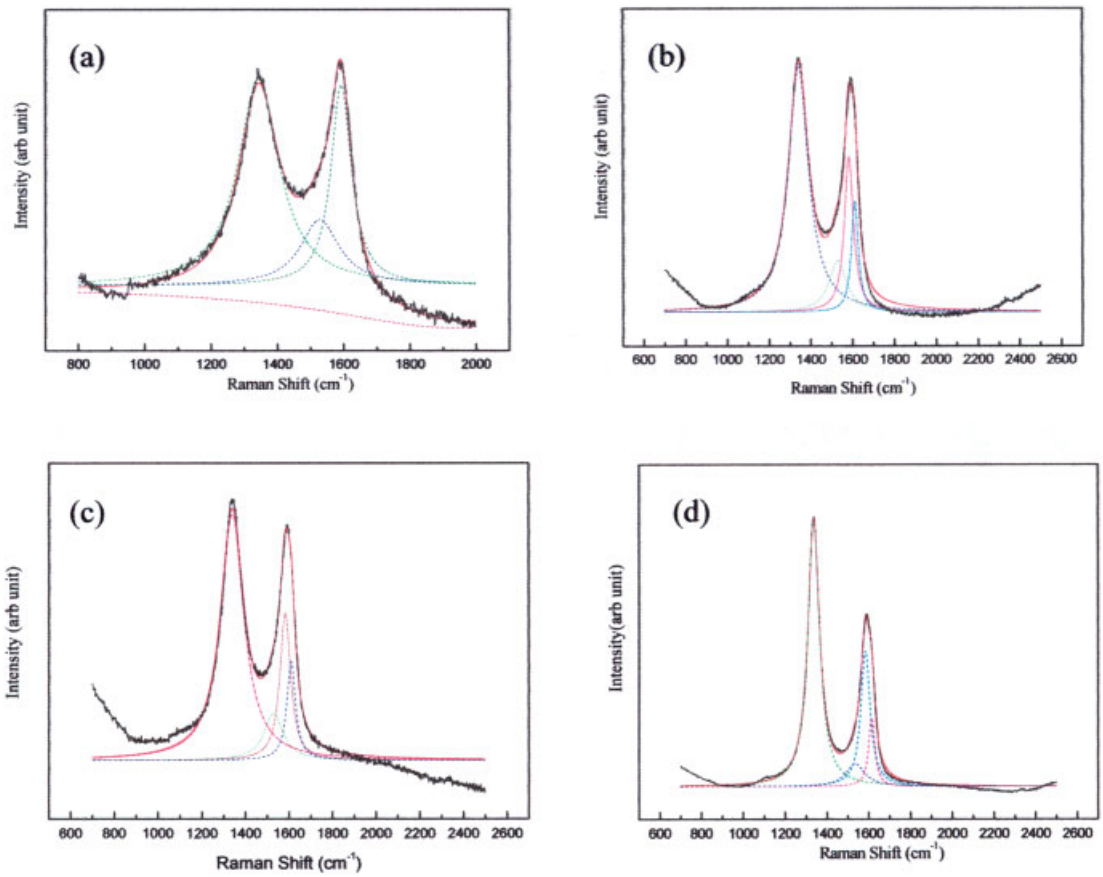

Figure 7 The result of fitted Raman spectra of various composites at the heat-treated temperature of 1000°C: (a) composite A, (b) composite B, (c) composite C, (d) composite D. [Color figure can be viewed in the online issue, which is available at www.interscience.wiley.com.]

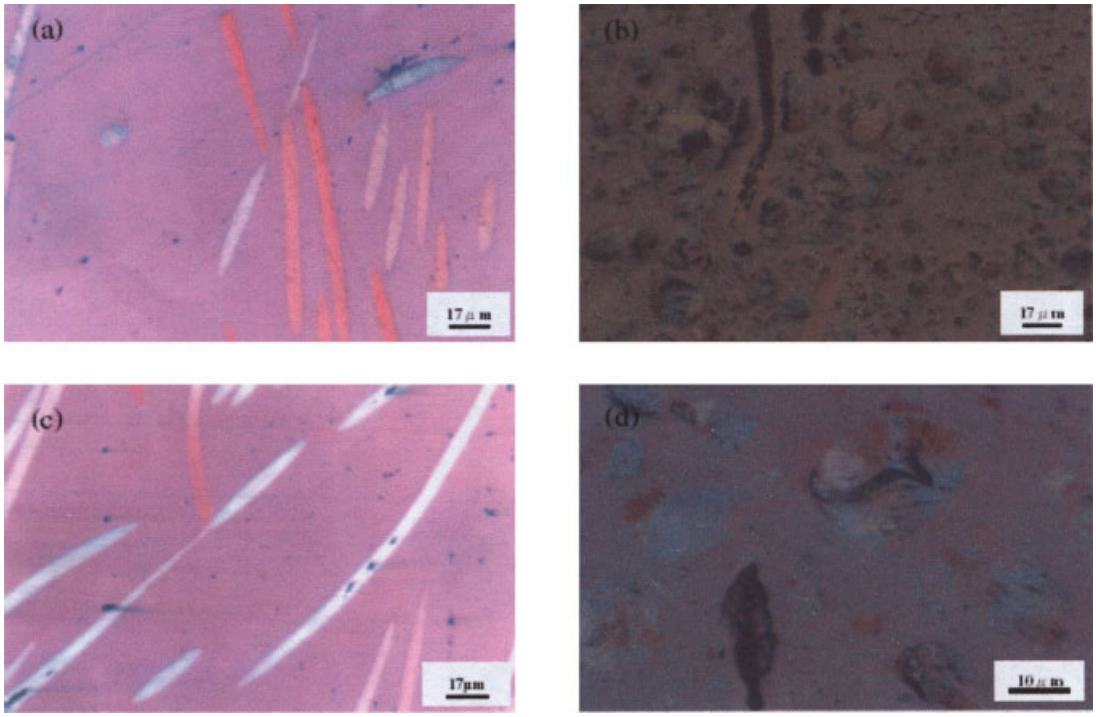

Figure 8 Polarized-light optical micrographs of carbon/carbon composites at different heat treatment temperatures: (a) composite A at 600°C, (b) composite D at 600°C, (c) composite A at 1000°C, (d) composite D at 1000°C. [Color figure can be viewed in the online issue, which is available at www.interscience.wiley.com.]

Optical microscopy

Polarized light is often used to observe interference color generated by orientation of graphitic lamellae at the surface.[28] Figure 8 plots the polarized-light optical micrographs of these C/C composites. Figure 8(a, c) for heat treatment at 600 and 1000°C respectively, reveal red or light red color in core of the fiber, which turns blue or light blue as heat-treatment temperature increases from 600 to 1000°C, indicating the fibers have an anisotropic texture and heat-treatment enhances preferred orientation of carbon. The matrix has an isotropic texture, as indicated by purple color in the matrix. MCMBs also revealed blue or light blue. They indicate anisotropic structure among MCMBs and fibers; indicate isotropic structures in phenolic resin matrix following pyrolysis. Matrix derived from phenolic resin is nongraphitizable carbon with glass- like isotropic texture. MCMBs and fibers is graphitizable carbon with anisotropy.

Mechanical properties, thermal conductivity, and electric resistance

Figure 9 plots variations in flexural strength of A, B, C, and D with temperature of heat-treatment. All composites exhibited maximal flexural strength after curing; the flexural strengths of polymer composites A, B, C, and D were 65.40, 60.34, 52.91, and 41.89 MPa, respectively. As the pyrolysis temperature rose from 230 to 400°C, the flexural strengths of various composites declined very rapidly to minimum. Above 400°C, flexural strength slowly increased again. Flexural strengths of composites A, B, C, and D were 51.20, 49.59, 43.55, and 38.76 MPa at 1000°C. Figure 10 plots flexural modulus of all composites against HTT; results are similar to that of flexural strength during pyrolysis. Still, maximal flexural modulus for all com-

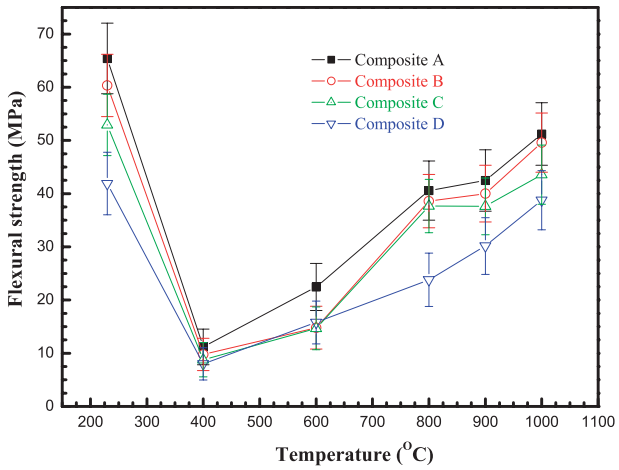

Figure 9 The change in the flexural strength of composites A, B, C, and D with heat treatment temperature in the range 230–1000°C. [Color figure can be viewed in the online issue, which is available at www.interscience.wiley.com.]

posites was observed at 1000°C; flexural modulus was 1.73 GPa for composite A, 1.24 GPa for B, 0.73 GPa for C, and 0.57 GPa for D.

At 400–600°C, flexural strength and modulus are low because of condensation of polymer structures in the resin[29] and crosslinks in oxidative PAN Base fiber felts. Above this temperature, abrupt increases in flexural strength for all composites are observed, due to repacking carbon basal planes in composites and enlarging carbon basal planes. Obviously, flexural strength and modulus of composites with MCMBs are lower than those of composite without MCMBs; this results from the voids and cracks around MCMBs caused by different shrinkage between MCMBs and resin, as shown in Figures 8(d) and 11(b).

Table III presents results of measuring thermal conductivity in a transverse direction of fibers and electric resistance. Clearly, thermal conductivity increases with amount of MCMBs added; at 1000°C, thermal conductivity of composite A is 1.55 W/mk; that of B is 1.57 W/mk, that of C is 1.57 W/mk, and that of D is 1.78 W/mk. electric resistance also reduces with amount of MCMBs added; electric resistance of composite A is 1.8×10^{-2} Ω cm; that of B is 6.7×10^{-3} Ω cm, that of C is 6.1×10^{-3} Ω cm, and that of D is 5.97×10^{-3} Ω cm.

CONCLUSIONS

The effect of adding MCMBs on microstructure, physical characteristics, electrical resistance, and thermal conductivity of C/C composites prepared by pyrolyzing oxidative PAN Base fiber felt/phenolic resin was gauged via heat treatment at 230–1000°C. Polarized-light optical microscopy, X-ray diffraction (L_C), and Raman spectroscopy (L_a) established differences between microstructures of the resin and MCMBs during cocarbonization: MCMBs and oxidative PAN Base fibers exhibit anisotropic texture, while phenolic matrix has an isotropic texture following carbonization. This trait shows how phenolic resin and MCMBs are nongraphitizable and graphitizable carbon, respectively. Adding MCMBs thus augments electrical resistance and thermal conductivity of carbon/carbon composites prepared from oxidative PAN Base fiber felt/phenolic resin. However the flexural strength and flexural moduli of composites with MCMBs added are lower than those without MCMBs below 1000°C; this fact may be associated with the strengthening of preferred orientation of a carbon layer plane with MCMBs added to composites. Composites with 30wt % MCMBs showed improvement in thermal (14.8%) and electrical conductivity (66.7%).

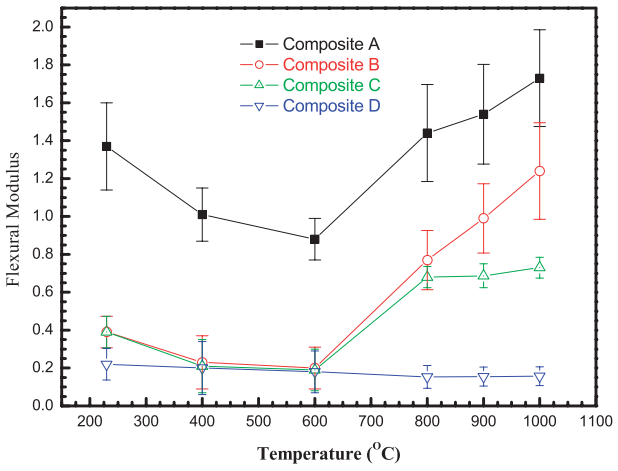

Figure 10 The change in the flexural modulus of composites R0, M10, and M30 with heat treatment temperature in the range 230–1000°C. [Color figure can be viewed in the online issue, which is available at www.interscience.wiley.com.]

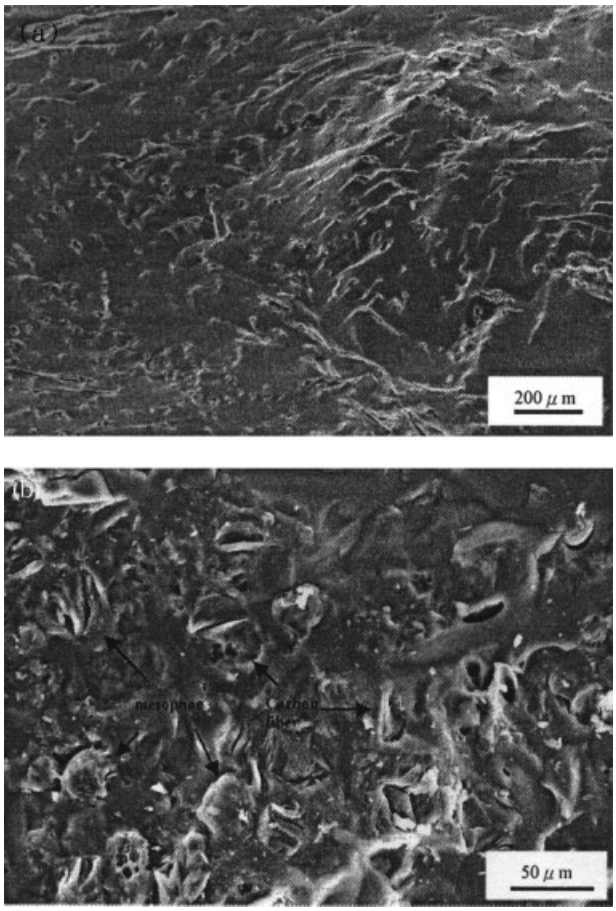

Figure 11 Morphology of fracture planes of composites after tree point bend test: (a) composites A after pyrolysis at 1000°C, (b) composites D after pyrolysis at 1000°C.

References

1. Hüttener, W. Carbon Fibers Filament and Composites; Kluwer Academic: Boston, 1990; p 275.

2. Fitzer, E. Carbon 1987, 25, 163.
3. Savage, G. Carbon–Carbon Composites; Chapman and Hill: London, 1993; Chapter 9.
4. Christel, P.; Meunier, A.; Dorlot, J. M. In Material Characteristics Versus in Vivo Behavior; New York Academy of Sciences: New York, 1988; Chapter 3.
5. Adam, D.; William, D. F.; Hill, D. F. J Biomed Mater Res 1978, 12, 35.
6. Manocha, L. M.; Manocha, S. M. Carbon 1995, 33, 435.
7. Morimoto, T.; Ogura, Y.; Konodo, M.; Ueda, T. Carbon 1995, 33, 351.
8. Yamanoto, O.; Sasamoto, O.; Inagaki, M. Carbon 1995, 33, 359.
9. Cheng, L. F.; Xu, Y. D.; Zhang, L. T.; Gao, R. Carbon 2000, 38, 2133.
10. White, J. L.; Shaeffer, P. M. Carbon 1989, 27, 697.
11. Lafdi, K.; Bonnamy, S.; Oberlin, A. Carbon 1991, 29, 831.
12. Nishizawa, T.; Sakata, M. Carbon 1992, 30, 147.
13. Brook, J. D.; Taylor, G. H. Nature 1965, 206, 697.
14. Brook, J. D.; Taylor, G. H. Carbon 1965, 3, 185.
15. Hoffmann, W. R.; Hüttener, K. J. Carbon 1993, 31, 259.
16. Wang, Y.-G.; Korai, Y.; Mochida, I. Carbon 1999, 37, 1049.
17. Hossain, S.; Kim, Y. K.; Saleh, Y.; Loutfy, R. J Power Sources 2003, 114, 264.
18. Tokumitsu, K.; Fujimoto, H.; Mabuchi, A.; Kasuh, T. Carbon 1999, 37, 1599.
19. Manocha, L. M.; Bhatt, H.; Manocha, S. M. Carbon 1996, 34, 841.
20. Ko, T. H. In Proceedings of the International Conference on Carbon, 1992; p 753.
21. Cullity, B. D. Element of X-ray Diffraction; Addison-Wesley: New York, 1978; p 99.
22. Lausevic, Z.; Marinkovic, S. Carbon 1986, 24, 575.
23. Fitzer, E.; Schafer, W.; Yamada, S. Carbon 1969, 7, 643.
24. Kimberly, A.; Trick, E.; Tony, E. Carbon 1995, 33, 1509.